Prediction of altered endograft path during endovascular abdominal aortic aneurysm repair with the Gore Excluder

David R. Whittaker, MD, Jeff Dwyer, BA, and **Mark F. Fillinger, MD,** *Lebanon, NH*

Objective: **During endovascular abdominal aortic aneurysm (AAA) repair (EVAR), the rapid deployment of the Gore Excluder endograft may be associated with anatomic shortening of the endograft path. This shortened path may result in coverage of the hypogastric artery origin or overly conservative graft length selection that may lead to unnecessary extensions. We quantified the degree of path alteration with this endograft and developed an algorithm to predict it.**

Methods: **Preoperative and postoperative three-dimensional (3D) computed tomographic (CT) scans were evaluated for 50 consecutive patients with Gore Excluder endografts by using 21 anatomic measurements and 6 calculated indices. Measurements were evaluated as if only 3D lumen centerline measurements were available, rather than complete 3D computer-aided measurement and "virtual graft" simulation. Tortuosity was quantitated from the renal artery to the hypogastric origin, using the difference between a straight line and the lumen centerline.**

Results: **The endograft was deployed successfully in all cases. The graft end points were typically quite close to the preoperative plan: mean renal artery-to-graft distance was within 2.0 ± .5 mm, and the limb end point-to-hypogastric origin differed by an average of only 1.8 ± 1.6 mm. Although accurate in most cases, the actual graft path shortened 1 cm or more relative to the centerline in 11% of limbs. On univariate analysis, determinants of alteration of >1 cm in the graft deployment path were (1) aortoiliac tortuosity (renal-to-hypogastric artery, $P < .002$), (2) the degree of planned graft rotation (73% of cases altered >10 mm were in the rotated position, $P < .05$), and (3) the insertion side (73% of alterations ≥10 mm were ipsilateral to the main device, $P < .05$). On multivariate analysis, the renal-to-hypogastric artery tortuosity index (RHTI) was significant ($P < .004$), and device type and rotation approached significance ($P < .08$). We developed a classification scheme based on RHTI to predict the risk of alteration of the graft path ≥1 cm (low risk, 0%; medium risk, 10%; high risk, 25%) and an algorithm to predict the degree of alteration of the anatomy that reduced the number of cases shortening ≥1 cm to zero.**

Conclusions: **The graft deployment path will be altered significantly in a minority of cases with the Gore Excluder endograft, but this can cause hypogastric occlusion or other problems. Anatomic shortening is predictable from morphologic features such as tortuosity, graft insertion side, and rotation. We developed an algorithm based on a tortuosity index that quantitates the risk and degree of shortening associated with endograft deployment. (J Vasc Surg 2005;41:575-83.)**

The Gore Excluder endograft (WL Gore & Associates) has been commercially available since 2002 and has been successfully placed in a large number of abdominal aortic aneurysms, encompassing a wide variation in morphology.[1,2] A unique characteristic of the Excluder is its rapid deployment mechanism. By pulling a release cord, the constrained self-expanding endoprosthesis is allowed to rapidly expand to its designed diameter, typically in ≤1 second. The standard deployment of the endoprosthesis includes a "super-stiff" guidewire. As with any device for endovascular repair, the combined guidewire, endoprosthesis, and delivery system may straighten tortuous anatomy to some degree. This straightening effect can thus result in the endograft taking a shorter path than planned and making the graft end point more distal than planned. With all devices, there is a tendency for at least partial elastic recoil of the aortoiliac arteries back to their original shape as the stiff delivery system is withdrawn. Our early experience with this particular device, however, suggested that in a minority of cases the rapid expansion and small delivery profile of this device might allow distal endograft fixation with the anatomy in a more straightened configuration than planned.

Typically, the small amount of straightening that occurs with this phenomenon can be easily predicted with preoperative planning based on three-dimensional (3D) computer-aided measurement, planning, and simulation (3D CAMPS) based on computed tomography (CT) or magnetic resonance scans.[3-5] In our series, length prediction with 3D CAMPS is very accurate and more accurate than using marker catheter angiography.[5] We have found this is true even if a "road-map" angiogram is performed, followed by insertion of a stiff guidewire into the marker catheter in an effort to take the shortening effect into account. Many centers still use less sophisticated 3D lumen centerlines alone, CT "angio" only, or marker catheters for length measurements, however (Fig 1).

From the Section of Vascular Surgery, Dartmouth-Hitchcock Medical Center.

Competition of interest: Jeff Dwyer is employed by Medical MetRx Solutions. Mark Fillinger receives research support from Medical MetRx Solutions.

Reprint requests: Mark F. Fillinger, MD, Dartmouth-Hitchcock Medical Center, One Medical Center Drive, Lebanon, NH 03756 (e-mail: Mark.Fillinger@Hitchcock.org).

0741-5214/$30.00

doi:10.1016/j.jvs.2005.01.033

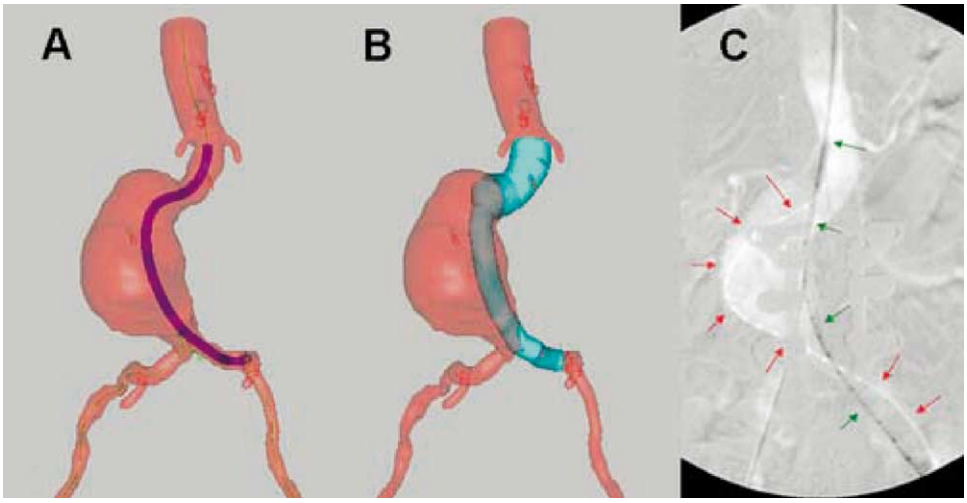

Fig 1. Comparison of length measurements with three-dimensional (3D) and angiographic marker catheter imaging, illustrating that multiple interpretations of the potential endograft path are possible. In **A,** the 3D lumen centerline length from the renal artery to the left hypogastric artery is 17 cm., whereas in **B,** the 3D user-defined path using "virtual graft" technique to account for the actual graft size is 15.8 cm. In **C,** the angiographic marker catheter length is 22 cm if the catheter is unconstrained but is only 14 cm if a stiff guidewire is placed within the marker catheter.

So although unexpected shortening in graft path is uncommon, it can result in two problems: (1) it can cause the device end point to end more distally and thus occlude a hypogastric artery, and (2) it can cause overly conservative device sizing, causing one to choose a shorter device in an effort to avoid inadvertent coverage of the hypogastric artery. The latter compensation, unfortunately, can also result in unnecessary extensions that may cost $2000 each, not to mention greater procedure time and the additional risk and potential durability issues of an unnecessary modular connection.

No matter what type of preoperative imaging is performed, some element of clinical judgment must always be applied to account for factors such as tortuosity (Fig 1). Although our group and others have found 3D CAMPS or similar technology to be more accurate[3-8] than marker catheter angiography, the prediction of the "virtual graft" path and especially "centerline-only" methods can still be improved, especially in tortuous anatomy. Because of apparent differences in devices, this may need to be studied in a device-specific manner. We studied clinical results with this endograft for two purposes: (1) to quantify the incidence and severity of graft path alteration with the Excluder device, and (2) to develop a mathematic algorithm to predict this alteration and thus to calculate a more optimal graft length on this basis.

METHODS

We reviewed 50 consecutive endograft placements (100 graft limbs) in patients who received Gore Excluder endografts at our institution between January 1999 and September 2003. The endografts in this study are a subgroup of 250 endovascular aortic aneurysm repairs during this time period. This study purposely includes devices placed during clinical trials with this device and thus includes the initial "learning curve" for the different investigators using the device at our institution. Data collection was approved by the institutional review board for human subjects.

Imaging. The primary preoperative imaging modality in all patients was spiral CT in conjunction with 3D reconstruction and Computer-Aided Measurement, Planning, and Simulation (3D CAMPS) software (Preview,® Medical Metrix Solutions, formerly Medical Media Systems, West Lebanon, NH). CT protocols were designed to image from the celiac artery to the femoral arteries, with good detail of branch vessels and adequate resolution for high-quality 3D reconstructions.[3,4,9] Contrast injection was at a rate of 3 to 4 mL/s (timed by CT monitoring or timing of a test bolus) and the iodinated contrast volume was typically 120 mL. For earlier generation scanners, collimation was typically 3 mm in the visceral aortic segment and 5 mm in the distal abdomen/pelvis, with a pitch of 1. More recently, collimation was typically 2.5 mm throughout. At all time points, reformats in the axial, sagittal, and coronal planes were in 2 mm increments, while reformats perpendicular to the vessel were 1 mm increments.

Clinically, the 3D CAMPS software was used for patient selection and device sizing, including standard preoperative measurements, "virtual graft" simulation to determine optimal graft rotation, and other key aspects of preoperative planning.[4,5] Intraoperative technique, including use of the 3D software for proper C-arm gantry positioning, has also been described previously.[4,5,10] Device deployment technique was according to the device instructions for use in all cases.

Study measurements. We used the 3D CAMPS software to perform 21 anatomic and graft measurements

Table I. Measurements and definitions

Measurement	*Type of measurement*	*Notes*
Renal to aortic bifurcation	Centerline	
Renal to aortic bifurcation	Straight line	
Renal to graft	Centerline	
Limb to hypogastric	Centerline	Left and right
Renal to hypogastric	Centerline	Left and right
Renal to hypogastric	Straight line	Left and right
Top of graft to limb end	Centerline	Left and right
Top of graft to limb end	Straight line	Left and right
Aortic bifurcation to hypogastric	Centerline	Left and right
Aortic bifurcation to hypogastric	Straight line	Left and right
Aortic neck angle (3D)	Angle	3D measurement
Iliac bifurcation angle (3D)	Angle	3D measurement
Top of graft to 20 mm distal	Centerline	
Top of graft to 20 mm distal	Straight line	
Renal to hypogastric	Calculated index	Centerline/straight line
Renal to hypogastric	Calculated index	Centerline – straight line
Renal to aortic bifurcation	Calculated index	Centerline/straight line
Renal to aortic bifurcation	Calculated index	Centerline – straight line
Aortic bifurcation to hypogastric	Calculated index	Centerline/straight line
Aortic bifurcation to hypogastric	Calculated index	Centerline – straight line

Aortic bifurcation, Defined by computed tomography (CT) reformat in which flow divider of aortic bifurcation first appears as a line; *Hypogastric (internal iliac artery)*, defined by CT reformat in which internal iliac artery clearly separates from external iliac artery (so it can be identified post-op also if the hypogastric was covered, intentionally or not); *Renal*, defined by CT reformat marking the inferior border of the lowest renal artery. *Top of graft*, defined by CT reformat in which the most proximal extent of the main body graft encompasses 50% or more of the lumen circumference; *Limb end*, defined by CT reformat in which the most distal extent of the iliac limb encompasses 50% or more of the lumen circumference. Start and endpoints for length measurements are defined as the center of the aorta in the orthogonal CT reformat that includes the stated anatomic feature. For both preoperative and postoperative data, the "path length" is defined from lowest renal artery to hypogastric on each side.

(Table I) on both the preoperative and postoperative CT scans. Length measurements were performed as if only lumen centerline measurements were available, however, and not by using the "virtual graft" simulation. To maintain uniformity, two reviewers adhered to the anatomic definitions for the measuring protocol. The reviewers' preoperative measurements for the study were compared with prospective 3D virtual graft simulations and clinic or operative notes to confirm that the actual graft placements were done in accordance with the preoperative plans (all were).

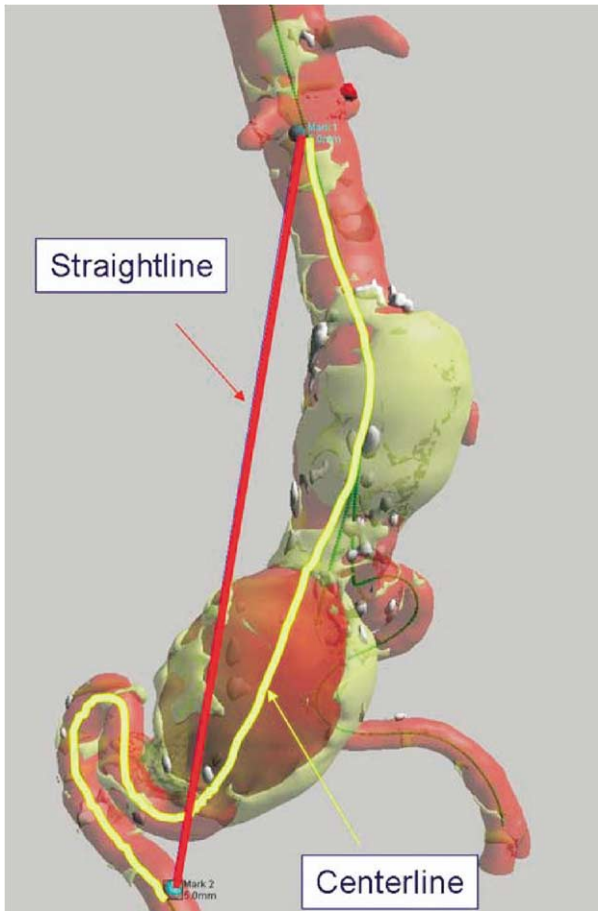

Fig 2. Example of measurements used to evaluate tortuosity. Shown here are 3D measurements for the renal artery-to-hypogastric artery tortuosity index (RHTI), where RHTI = (lumen centerline length – straight line length) as measured from the center of the aorta just below the lowest renal artery to the center of the common iliac artery just proximal to the hypogastric artery origin. The other tortuosity indices are calculated in similar fashion as described in Table I.

In addition to standard anatomic measurements, we prospectively formulated six different indices of tortuosity to evaluate a possible association with graft path alteration, consistent with proposed standards.[11] These indices are defined in Table I and Fig 2. To account for the potential variability produced by the structural differences in the ipsilateral main device and contralateral limbs of the endograft, all graft path measurements were identified as either ipsilateral (main device) or contralateral (contralateral limb). Because the graft can be purposely rotated to facilitate cannulation of the contralateral limb, the orientation and degree of rotation for each limb were recorded in 90-degree increments. The "standard" configuration was defined as positioning of the contralateral docking limb to

maximize the apparent distance from the ipsilateral limb in a "standard" posteroanterior fluoroscopic projection.

The postoperative measurements were performed for the actual graft path seen on the CT. For both preoperative and postoperative data, the "path length" was defined from lowest renal artery to the hypogastric on each side (Table I) to avoid confounding issues related to distance from the renal artery to the top of the graft after placement. The actual centerline path including the endograft, as determined on CT, was compared with the actual preoperative lumen centerline (not the virtual graft simulation). It is important to note that in many cases, the preoperative plan was designed to take advantage of a graft path shorter than the centerline path, including a "user defined graft path"[4,9] or purposely rotating the endograft away from the "standard" rotation, or both, to intentionally shorten one limb or lengthen the opposing limb (Fig 3).[5] For the sake of the study, however, any shortening of the path relative to the lumen centerline was considered to be "shortening," even if it was created intentionally or accounted for in the preoperative plan.

Statistical analysis. Anatomic measurements were analyzed using Statview, a standard statistical software package (SAS Institute, Cary, NC). Nominal variables were compared by χ^2 or the Fisher exact test. Continuous variables were analyzed using analysis of variance (ANOVA), and linear regression was used to evaluate potential correlation between preoperative measurements and graft path alteration. Multivariate logistic regression analysis was performed to evaluate variables that were significant by univariate analysis.

RESULTS

Technical success and device placement. The endograft was successfully deployed in all 50 patients (100 limbs). Device deployment was generally quite accurate, with the distance from the renal artery to the top of the graft on the postoperative CT scan $\leq 2.0 \pm .5$ mm of the planned deployment location. One graft was unintentionally deployed 14 mm below the renal arteries, resulting in the only aortic cuff and the only unplanned device extension in the series. There were 19 planned iliac limb extensions and 16 limbs planned to extend into the external iliac artery for complete aneurysm exclusion. In those limbs where the hypogastric was not intentionally covered, the average final distance between the end of the graft limb and the hypogastric origin was $\leq 1.8 \pm 1.6$ mm of the planned position (0.4 ± 1.5 mm if including limbs with extensions). Inadvertent coverage of hypogastric arteries occurred in two patients, and in one of the two cases was due to deployment of the device 14 mm below the renal arteries, rather than 2 mm as planned. Three of 100 hypogastric arteries were inadvertently covered, with no sequelae in one patient and spontaneously resolving claudication in the patient with bilateral coverage. There were no attachment site or device junction endoleaks at completion or follow-up.

Anatomic data and univariate analysis. The results for anatomic measurements are listed in Table II, including ANOVA and linear regression to evaluate potential correlation between anatomic measurements and graft path alteration (specifically, shortening of ≥ 10 mm for ANOVA). With regard to these patient-specific anatomic variables, only tortuosity of the native anatomy was significantly associated with the degree of postoperative path alteration (Table II). Of the six tortuosity indices, the renal-to-hypogastric tortuosity indices demonstrated the best correlation with alterations in the graft path, as summarized in Table III.

The change in the distance from the lowest renal artery to the hypogastric artery (centerline preoperative – actual postoperative) averaged $3.2 \pm .7$ mm. The actual postoperative graft path was 10 mm shorter than the preoperative centerline path in 11% of limbs. Differences of this degree appeared to be associated with both the degree of the planned graft rotation (73% of these cases were in the rotated position, $P < .02$, χ^2) and with the main device (73% of these cases were ipsilateral to the main device, $P < .05$). When evaluating these factors in combination, the limbs associated with *both* main device *and* graft rotation were more likely to have a shorter postoperative path (mean, 7.2 ± 1.8 mm) than those with characteristics of main device-standard position (1.5 ± 0.9 mm), contralateral limb-standard position (2.8 ± 0.8 mm), or contralateral limb-rotated (2.6 ± 2.4 mm), $P < .03$ ANOVA.

It was also uncommon for the actual postoperative graft path to take a *longer* route than the preoperative centerline path, as the actual graft path was only 5 mm longer than the preoperative centerline in 8% of limbs. Limbs taking a longer path were also associated with the limb type and graft rotation, as 75% of these were contralateral limbs and 75% were rotated from standard position ($P < .05$). Thus, graft rotation from the standard position appeared to be associated with altered path in general (shorter or longer), whereas the main device appeared to be more specifically associated with a shorter path.

Multivariate analysis. Factors that appeared to be associated with graft path alteration on univariate analysis were then input into a multivariate logistic regression model for graft path alteration of ≥ 10 mm. In this analysis, the only significant variable was related to the degree of tortuosity. The renal-to-hypogastric tortuosity index (RHTI) was the best of the tortuosity indices ($P < .004$), as defined in Table I and shown in Fig 2. Combining the variables for device (main device vs contralateral limb) and for graft rotation (rotated vs "standard" position) into a single variable for "limb type and rotation" resulted in a single variable that approached significance in the multivariate analysis ($P < .08$), but did not improve the model statistically.

Categorization of risk-predictive algorithm. Tortuosity was thus used to assess a potential risk-prediction strategy. The population in this study was subdivided based on the RHTI calculated as 3D centerline distance – 3D straight-line distance (Fig 2). A simple categorization method was created, with the limbs grouped into three categories of risk for an altered graft path: low risk (RHTI

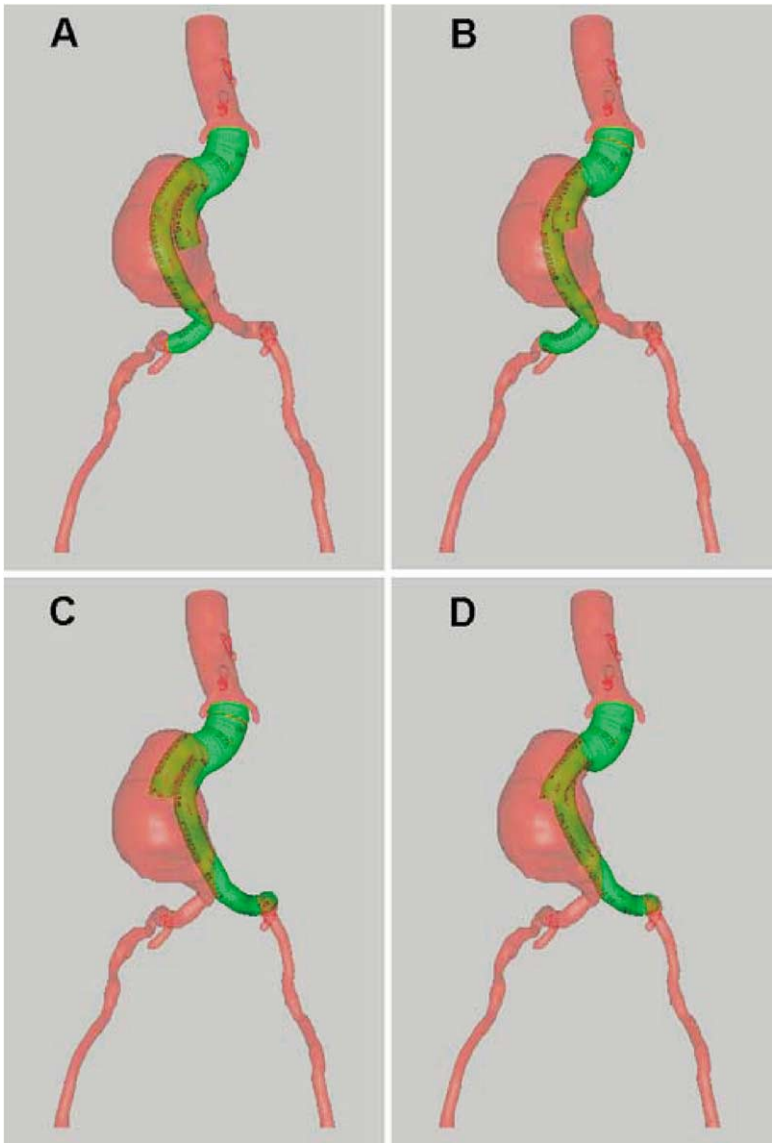

Fig 3. Virtual graft simulation to demonstrate the potential effect of endograft rotation and insertion site for the main device (trunk and ipsilateral limb). Configurations shown are **A,** main device inserted via right with docking limb in standard contralateral position; **B,** main device inserted via right with docking limb rotated 90 degrees, to an anterior position; **C,** main device inserted via left with docking limb in standard contralateral position; **D,** and main device inserted via left with docking limb rotated 90 degrees, to an anterior position. The device length is the same in each simulation, but has different endpoints because of the side of insertion and rotation. A shorter device should be chosen in each case and illustrates the utility of simulating the endograft insertion side, length, diameter, and amount of rotation within the anatomy rather than constraining the simulation rigidly to the centerline. Configurations **B** or **D** are preferred in this case, as they allow the device to bend along its most flexible axis. The configuration shown in **A** might compress the docking limb and collapse it before cannulation, and the configuration shown in **C** would make cannulation of the docking limb much more difficult. Device length would be adjusted to account for the chosen configuration and where the device will be deployed relative to the renal arteries.

<21 mm), medium risk (RHTI, 21 to 39 mm), and high risk (RHTI >39 mm). Of the 100 limbs, 25 were considered low risk, 55 were medium risk, and 20 were high risk. The risk of a path "shortened" ≥10 mm or more was low risk, 0%; medium risk, 10%; and high risk, 25%.

RHTI and linear regression data were used to create an algorithm to predict the degree of graft path alteration (Table IV). Using the preoperative 3D centerline only, the graft path length "error" (predicted – actual) was 8.1 ± 2 mm in the high-risk group (the actual path was shorter,

Table II. Anatomic data

Measurement	*Type of measurement*	*Mean*	*SE*	P*	P†
Renal to aortic bifurcation	Centerline, mm	125	2	.14	.2
Renal to aortic bifurcation	Straight line, mm	115	2	.7	.9
Renal to Graft, pre-op	Centerline	0.6	.2	.9	.8
Aortic bifurcation to hypogastric	Centerline	61	2	.8	.7
Aortic bifurcation to hypogastric	Straight line	58	1	.4	.2
Top of graft to limb end	Centerline	170	2	.3	.3
Top of graft to limb end	Straight line	144	2	.3	.2
Renal to hypogastric	Centerline	185	2	.15	.2
Renal to hypogastric	Straight line	154	2	.4	.1
Aortic neck angle (3D)	Angle, degrees	21	1	.1	.1
Top graft to 20 mm distal, pre	Straight line	20.6	.5	.7	.3
Limb end to hypogastric	Centerline	15	2	.6	.9
Iliac bifurcation angle (3D)	Angle, degrees	78	2	.2	.2
Renal to aortic bifurcation	Centerline/straight line	1.1	.01	.001	.01
Renal to aortic bifurcation	Centerline–straight line	10	.7	<.001	.01
Aortic bifurcation to hypogastric	Centerline/straight line	1.1	.01	.14	.02
Aortic bifurcation to hypogastric	Centerline–straight line	3.9	.5	.13	.01
Renal to hypogastric	Centerline/straight line	1.2	.01	.002	<.0001
Renal to hypogastric	Centerline–straight line	31	1.2	.002	<.0001
Postoperative values					
Renal to graft, postop (half circ)	Centerline	2.5	.4	.1	.01
Change renal-graft (pre-post)	Centerline	−2.0	.5	.25	.1
Change in neck angle postop	Angle, degrees	−0.8	.7	.4	.7
Change in iliac angle postop	Angle, degrees	−0.5	2	.1	.2
Change in renal to hypogastric	Straight line	−1.4	.4	.6	.7
Change in renal to hypogastric	Centerline	3.2	.7	NA‡	NA

**P* value for the analysis of variance (ANOVA) statistic, with the nominal variable dividing the limbs into groups by degree of shortening (shortening by ≥10 mm).
†*P* value for a linear regression of the variable versus *Change in renal to hypogastric, centerline* length (preoperative centerline – actual postoperative path).
‡*Change in renal to hypogastric*, *centerline* is the outcome measure used as the reference for statistical calculations.

Table III. Linear regression results for three-dimensional tortuosity indices

Measurement	*Index or ratio*	P	R	r^2
Renal to hypogastric	Centerline/straight line	<.0001	.45	.21
Renal to hypogastric	Centerline – straight line	<.0001	.44	.19
Renal to aortic bifurcation	Centerline/straight line	.01	.26	.07
Renal to aortic bifurcation	Centerline – straight line	.01	.28	.08
Aortic bifurcation to hypogastric	Centerline/straight line	.02	.25	.06
Aortic bifurcation to hypogastric	Centerline – straight line	.01	.26	.07

Results are for linear regression of the described tortuosity index versus the degree of graft path alteration as defined in the text. Measurement definition is the same as other Tables.

thus causing the graft endpoint to be more distal than expected). By applying a corrective algorithm based on RHTI, the predicted graft position was modified such that the actual path would end with the distal graft 1.1 ± 2 mm *proximal* to the predicted location in the high-risk group, rather than 8.1 mm *distal* to the predicted location (Table IV).

To investigate the potential utility of adding other factors into the algorithm, a second algorithm was created to take graft rotation into account. Table IV also displays the percentage of limbs that would have an actual graft path length ending 1 cm more distal or 1 cm more proximal than predicted. As shown, both algorithms reduce the chances that the graft path will err by ≥1 cm, and are more conservative than the centerline path (ie, having no cases with a predicted path 1 cm "too long" makes it unlikely that a hypogastric might be covered inadvertently). Our use of 3D CAMPS with virtual graft simulation appears to have a similar effect (Table IV), although prospective virtual graft plans were only available for 40 of 50 cases.

DISCUSSION

In this study, we found that the endograft deployment path will be altered significantly in a minority of cases with the Gore Excluder endograft. Although this straighter endograft path infrequently differs by >1 cm from the 3D lumen centerline path, the effect of a more-distal-than-planned stent-graft end point can cause hypogastric occlusion in the most extreme cases. Fortunately, it appears that this straightening of the anatomy is predictable from ana-

Table IV. Prediction algorithm results

Method to Assess Graft Path Length (results in mm)	*Low risk N = 25*	*Med risk N = 55*	*High risk N = 20*	P*	*Actual ends 1 cm distal†*	*Actual ends 1 cm prox†*
Preop centerline – actual path	1.8 ± 1	2.1 ± 1	8.1 ± 2	.003	11%	3%
Algorithm 1, predicted – actual path	1.6 ± 1	−1.7 ± 1	−1.1 ± 2	.3	2%	5%
Algorithm 2, predicted – actual path	0.8 ± 1	−2.9 ± 1	−3.4 ± 2	.1	0%	9%
Centerline to end of virtual graft‡	6.2 ± 4	16 ± 2	23 ± 2	<.01	2%	0%

Algorithm 1 = 3D centerline – [(RHTI × 0.266) − 4]; Algorithm 2 = 3D centerline − [(RHTI × 0.266) − 4 + (3.4 if graft is rotated)], where *RHTI* (renal to hypogastric tortuosity index) is "renal-to-hypogastric, centerline – straight line" as defined previously.

*ANOVA for the degree of difference in path length for the various methods versus risk stratification (low, medium, high).

†Percentage of patients who would have an actual graft path length ≥1 cm shorter than predicted (thus the graft endpoint is more distal than predicted) or ≥1 cm longer than predicted (thus the graft endpoint is more proximal than predicted).

‡Centerline measurements do not account for our clinical use of a user-defined virtual graft path simulation or purposely taking advantage of path shortening by rotating the graft, which is accounted for in the final row of the table. This row demonstrates a significant difference between the centerline end point and the simulated virtual graft end point, greater in the higher-risk groups. Thus the virtual graft simulation can also identify the risk, and only 2% of grafts ended 1 cm different than predicted when virtual graft was used.

tomic features that are identifiable preoperatively. It also appears that the shortening affect is much more heavily influenced by anatomic factors than by device factors.

Although the effect of graft path shortening due to stiff guidewires and delivery systems may be well known clinically, it has received little attention in the literature. Several studies have investigated alterations in graft path or aortic length after endovascular abdominal aortic aneurysm repair (EVAR), but almost all of these investigate changes over long time periods caused by aneurysm sac changes.

White et al[12] studied acute graft path alterations at the time of deployment with 39 Vanguard (Boston Scientific) and 25 AneuRx (Medtronic) devices, suggesting that these devices tended to have an end point more proximal than one would expect rather than more distal. Using graduated marker catheter angiography for length measurements, they found graft length end point differences of ≥15 mm in 56% of the Vanguard and in 44% of the AneuRx endografts. Additional extensions were required to correct endoleak caused by inadequate graft length in 14% of patients.

One potential explanation for the findings of White et al is the use of marker catheter angiography for preoperative length measurements. Although standard at the time of that study and still used in many centers, we have found that marker catheter angiography is not as accurate as the 3D CT lumen centerline or more advanced technology like 3D CAMPS. In prospective comparisons of 3D CAMPS and marker catheter angiography for EVAR, we found them to differ by >1 cm in 19% of limbs and 3D CAMPS to be more accurate in each case.[3-5] Our initial validation cases also included AneuRx and Vanguard devices identical to those cited in the study of White et al.

We have eliminated the need for preoperative marker catheter angiography since 1996 by using 3D CAMPS, with excellent results for a wide variety of endografts, in the largest series using 3D CAMPS to prospectively determine endograft length and diameter to date.[5] With a single exception using a different system,[14] other smaller series have also confirmed that 3D CAMPS (or similar technology) is equivalent or superior to marker catheter angiography.[6-8,13,15,16] Thus, the discrepancy in endograft path length issues is more likely imaging-related rather than device-related in this case.

Despite the accuracy of 3-D CAMPS, we are constantly seeking improvement or automation, or both, especially for "exception" cases at the extremes of typical anatomy. Initially, as we helped develop 3D CAMPS and virtual graft simulation, we would evaluate both the centerline path and what we have described as a "user-defined" path when we thought the endograft might not follow the centerline (Fig 1).[3-5] After numerous cases, we found that the "user-defined path" was usually shorter than the centerline path, but the differences were small, typically ≤5 mm. After the first 100 cases, we performed the "user-defined path"[4,5] only for atypical cases with more tortuous anatomy, as it is somewhat tedious to perform.

Tillich et al[17] used 3D imaging to evaluate preoperative and postoperative stent-graft length in 31 AneuRx and 2 Excluder stent-grafts. They suggested that the stent-graft path is best predicted by the shortest 3D aortoiliac path length maintaining at least one iliac radius distance from the vessel wall, with a mean error of 2.1 mm ± 4.6 mm. Their results are similar to the mean value in the present study using 3D lumen centerline measurements. However, even a lumen centerline path will be shorter than the actual graft path in some cases (Table IV), so the routine use of a "shortest possible" path is not an ideal solution.

Thus, the key is to know when significant straightening of the anatomy is likely and then to select the endograft length appropriately. In this regard, awareness of the key risk factors or a predictive algorithm, or both, should improve the accuracy of deployment and clinical results. Of course, the importance of tortuosity is obvious, and some might believe it is a simple matter to evaluate tortuosity on CT or angiography. We believe that quantifying the associated graft path alteration will be helpful, however.

It is a simple matter to determine that the anatomy is "tortuous," but estimating the stent-graft endpoint is not trivial, especially for device-specific issues. Wolf et al,[18] reported that increased tortuosity was associated with

longer fluoroscopy time, more contrast, use of extensions, arterial reconstruction, and endoleak. We had no arterial reconstructions or type I endoleak, and 16 of 19 extensions in this study were required because of planned end points in the external iliac, so we cannot readily compare the two experiences. Nevertheless, this points out the importance of tortuosity in terms of case planning and patient selection for EVAR.

It is also important to note potential risk factors for an altered graft path that can be controlled by the implanting physician. Endograft rotation is perhaps the most difficult of these factors to predict, especially without access to 3D CAMPS. In some cases, rotation away from the standard position will shorten the actual graft path, whereas in others, it will lengthen it (Fig 3). This points out why simple mathematic algorithms cannot replace the combination of an accurate representation of the 3D anatomy and experienced clinical judgment. We frequently plan graft rotation to purposely shorten the actual graft path, to allow the device to bend along a more natural axis, or to make cannulation of the docking limb easier.[4,5,10]

The trunk-ipsilateral limb deployment system may also be a risk factor for a straightened graft path due to its stiffness and length (in comparison with the contralateral limb). By using 3D CAMPS and virtual graft simulation, case planning strategy becomes much more obvious (Fig 3). For the actual case plans in this series using 3D CAMPS, we planned a shorter path than the centerline for the more tortuous cases (Table IV). This verifies our impression that virtual graft simulation, which includes simulation of the endograft diameter, is quite accurate, but incorporating the data from this study may improve these simulations further.

Finally, the cases with hypogastric coverage in this series involved less experienced users, and experience clearly impacts EVAR results in general.[19,20] For example, the main device may be deployed more distally than originally planned, causing the distal end point to end more distally than planned. We have found that using 3D CAMPS to correct the C-arm gantry position for the aortic "neck" assists greatly in proper device placement immediately below the renal arteries.[10] Gantry angle correction alone can cause errors of >1 cm in graft deployment and should be accounted for.[4,21] Our results in this series for device placement relative to the renal arteries are quite good, in part because of gantry correction. In one case with hypogastric occlusion in this series, the plan accounted for shortening, but not adequately, in anatomy that is now known to be more than two standard deviations from the mean by tortuosity index. We believe these learning curve issues can be overcome, or at least improved, with imaging technology.

One might argue that the solution to graft path alterations is to use "conservative" device sizing, choosing a shorter device in an effort to avoid inadvertent coverage of the hypogastric artery. This compensation, unfortunately, can result in unnecessary extensions that may cost $2,000 each, not to mention greater procedure time, additional risk, and potential durability issues of an unnecessary modular connection. The goal of EVAR should be to minimize the number of extensions, the inadvertent coverage of a hypogastric artery, and the incidence of endoleak. In this series, there were no type I endoleaks, and 28% of patients had extensions, compared with 40% in the most recent Gore Excluder trial.[22] This is consistent with findings of our center and others that 3D CAMPS results in less extensions than marker catheter angiography.[8,23] The percentage of inadvertent hypogastric coverage was not reported in the Excluder trial, but the rate in this study compares favorably to the rate of 3% to 10% in the literature.[23] Our multiple-device series also has one of the lowest reported rates of inadvertent hypogastric coverage at 1.5%.[23]

Conclusion. The graft deployment path will be altered significantly in a minority of cases with the Gore Excluder endograft, but anatomic shortening is predictable. We developed an algorithm that quantitates the risk and degree of shortening associated with endograft deployment, which will need to be validated prospectively on an independent dataset.

REFERENCES

1. Matsumura JS, Brewster DC, Makaroun MS, Naftel DC. A multicenter controlled clinical trial of open versus endovascular treatment of abdominal aortic aneurysm. J Vasc Surg 2003;37(2):262-271.
2. Leurs LJ, Hobo R, Buth J. The multicenter experience with a third-generation endovascular device for abdominal aortic aneurysm repair. A report from the EUROSTAR database. J Cardiovasc Surg (Torino) 2004;45(4):293-300.
3. Fillinger MF. Utility of spiral CT in the preoperative evaluation of patients with abdominal aortic aneurysms. In: Whittemore AD, editor. Advances in Vascular Surgery, Vol 5. St. Louis, MO: Mosby; 1997. p. 115-131.
4. Fillinger MF. New imaging techniques in endovascular surgery. Surg Clin North Am 1999;79(3):451-475.
5. Wyers M, Fillinger M, Schermerhorn M, Powell R, Rzucidlo E, Walsh D, et al. Endovascular repair of abdominal aortic aneurysm without preoperative arteriography. J Vasc Surg 2003;38(4):730-738.
6. Broeders IA, Blankensteijn JD, Olree M, Mali W, Eikelboom BC. Preoperative sizing of grafts for transfemoral endovascular aneurysm management: a prospective comparative study of spiral CT angiography, arteriography, and conventional CT imaging. J Endovasc Surg 1997;4(3):252-261.
7. Sprouse LR 2nd, Meier GH 3rd, Parent FN, DeMasi RJ, Stokes GK, LeSar CJ, et al. Is three-dimensional computed tomography reconstruction justified before endovascular aortic aneurysm repair? J Vasc Surg 2004;40(3):443-447.
8. Velazquez OC, Woo EY, Carpenter JP, Golden MA, Barker CF, Fairman RM. Decreased use of iliac extensions and reduced graft junctions with software-assisted centerline measurements in selection of endograft components for endovascular aneurysm repair. J Vasc Surg 2004;40(2):222-227.
9. Fillinger MF. Computed tomography, CT angiography and three-dimensional reconstruction for the evaluation of vascular disease. In: Rutherford RB, editor. Rutherford's Textbook of Vascular Surgery, Fifth ed. Philadelphia, PA: W. B. Saunders; 1999.
10. Fillinger MF, Weaver JB. Imaging equipment and techniques for optimal intraoperative imaging during endovascular interventions. Semin Vasc Surg 1999;12(4):315-326.
11. Chaikof EL, Fillinger MF, Matsumura JS, Rutherford RB, White GH, Blankensteijn JD, et al. Identifying and grading factors that modify the outcome of endovascular aortic aneurysm repair. J Vasc Surg 2002; 35(5):1061-1066.
12. White GH, May J, Waugh R, Harris JP, Chaufour X, Yu W, et al. Shortening of endografts during deployment in endovascular AAA repair. J Endovasc Surg 1999;6(1):4-10.

13. Beebe HG, Kritpracha B, Serres S, Pigott JP, Price CI, Williams DM. Endograft planning without preoperative arteriography: a clinical feasibility study. J Endovasc Ther 2000;7(1):8-15.
14. Brown WA, Miller R, Birch S, Scott A. Is aortic angiography necessary for accurate planning of endovascular aortic aneurysm stents? Cardiovasc Surg 2003;11(1):1-5.
15. Aziz I, Lee J, Lee JT, Donayre CE, Walot I, Kopchok G, et al. Accuracy of three-dimensional simulation in the sizing of aortic endoluminal devices. Ann Vasc Surg 2003;17(2):129-136.
16. Coenegrachts K, Rigauts H, De Letter J. Prediction of aortoiliac stent graft length: comparison of a semiautomated computed tomography angiography method and calibrated aortography. J Comput Assist Tomogr 2003;27(2):284-288.
17. Tillich M, Hill BB, Paik DS, Petz K, Napel S, Zarins CK, et al. Prediction of aortoiliac stent-graft length: comparison of measurement methods. Radiology 2001;220(2):475-483.
18. Wolf YG, Tillich M, Lee WA, Rubin GD, Fogarty TJ, Zarins CK. Impact of aortoiliac tortuosity on endovascular repair of abdominal aortic aneurysms: evaluation of 3D computer-based assessment. J Vasc Surg 2001;34(4):594-599.
19. Laheij RJ, van Marrewijk CJ, Buth J, Harris PL. The influence of team experience on outcomes of endovascular stenting of abdominal aortic aneurysms. Eur J Vasc Endovasc Surg 2002;24(2):128-133.
20. Forbes TL, DeRose G, Kribs SW, Harris KA. Cumulative sum failure analysis of the learning curve with endovascular abdominal aortic aneurysm repair. J Vasc Surg 2004;39(1):102-108.
21. Broeders IA, Blankensteijn JD. A simple technique to improve the accuracy of proximal AAA endograft deployment. J Endovasc Ther 2000;7(5):389-393.
22. Gore. Excluder Instructions for Use. 2004.
23. Wyers MC, Schermerhorn ML, Fillinger MF, Powell RJ, Rzucidlo EM, Walsh DB, et al. Internal iliac occlusion without coil embolization during endovascular abdominal aortic aneurysm repair. J Vasc Surg 2002;36(6):1138-1145.

Submitted Oct 25, 2004; accepted Jan 26, 2005.